

# Enhanced FT for Orbitrap Mass Spectrometry

Oliver Lange, Eugen Damoc, Andreas Wiegghaus, Alexander Makarov

Thermo Fisher Scientific, Bremen, Germany

## Overview

**Purpose:** Increase resolving power of Orbitrap™ analyzer at a given acquisition time.

**Methods:** Enhancement of Fourier transformation (eFT™) was developed.

**Results:** Resolving power is typically doubled for the same acquisition time.

## Introduction

The Fourier transformation of the time-domain transient provides a complex value for each point in the frequency domain (a complex spectrum). Complex values are usually represented as pairs of magnitude and phase or as real (Re) and imaginary (Im) components.

By making use of the phase information, an 'absorption' spectrum and a 'dispersion' spectrum can be calculated from the real component and the imaginary part of the spectrum [1-2]. However, in general, real and imaginary components produce asymmetric peak shapes, except for special cases, e.g. when the phase of that peak is zero (Fig. 1). FTMS data systems have, therefore, conventionally neglected the phases and used the so-called 'magnitude' spectrum given by the following:

$$M(p) = \sqrt{\text{Re}(p)^2 + \text{Im}(p)^2} \quad (1)$$

where  $M(p)$  is the magnitude value at a point  $p$  in the frequency ( $f$ ) domain;  $\text{Re}(p)$  is the real component from the Fourier transformation at the point  $p$ ; and  $\text{Im}(p)$  is the imaginary component from the Fourier transformation at the point  $p$ . The  $m/z$  value can be derived from the frequency  $f$ . The use of the magnitude spectrum, which amounts to disregarding the phase information, yields symmetrical peaks in frequency and mass spectra but suffers from reduced resolving power compared to the pure absorption spectrum, by a factor between 1.4 and 2 [1].

Additional broadening of peaks comes from further processing of spectra such as apodization, i.e. windowing of the transient to improve a peak shape.

- Transfer from traditional magnitude presentation of mass spectra to real component presentation improves an increase of resolving power up to 2x.
- Such transfer could be possible only if phase information in the spectrum is taken into account.

## Methods

### Synchronization of Ions in Orbitrap Analyzers

Orbitrap mass spectrometers differ fundamentally from most FT ICR mass spectrometers by their built-in excitation-injection mechanism [3]. In short, a quasi-continuous ion beam enters a gas-filled C-trap (Fig. 2) where ions collide with bath gas, lose energy and get cooled. After RF is ramped down, radial DC is applied across rods, and ions are ejected along lines converging on the Orbitrap entrance. As ions enter the Orbitrap analyzer as small packets, increasing voltage on the central electrode causes ions, at the same time forcing them to move towards the center of the trap and thus exciting axial oscillations.

- A) Initial phase 0 degrees
- B) Initial phase -45 degrees

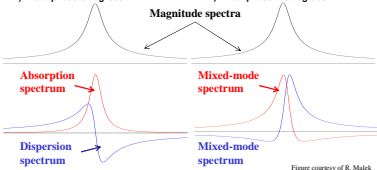


Figure courtesy of R. Malek

**FIGURE 1. A)** Absorption and dispersion spectra resulting from Fourier transformation when signal phase is 0° at the start of the transient (i.e. pure cosine), and **B)** mixed-mode spectra resulting from FT when signal phase is -45° at the start of the transient [1, 2, 4]. In both cases, transient with a substantial exponential decay was chosen in order to minimize Gibbs oscillations [4].

Time-of-flight from the C-trap to the Orbitrap is proportional to  $(m/z)^{1/2}$

$$t_{\text{tof}} = \frac{L_{\text{eff}}}{\sqrt{\frac{2eV}{m \cdot z}}} \quad (2)$$

while axial frequency is proportional to  $(m/z)^{-3/2}$ , so the phase acquired by ions traveling along effective length  $L_{\text{eff}}$  from the C-trap to the Orbitrap analyzer, becomes mass-independent in the first-order approximation:

$$\Delta\varphi = \omega \cdot t_{\text{tof}} = \frac{L_{\text{eff}}}{2k} \cdot \omega^2 = \text{const} \quad (3)$$

This simple phase relationship enables the calculation of the absorption spectrum in a straightforward manner, however a precise synchronization of detection to the initial starting moment  $t_0$  is needed [3]. This moment is defined by extrapolating detected signals in time-domain back in time to the point where their phase difference is minimized. For best results, the detection needs to start as early as possible after ion injection. Modifications to the preamplifier and Orbitrap designs were introduced in order to reduce the delay of starting transient detection from almost 10 ms to a fraction of a millisecond (Fig. 4).

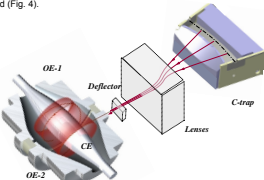


**FIGURE 2.** Scheme of coupling of the C-trap to the Orbitrap analyzer resulting in excitation-by-injection and synchronization of ion motion. OE denotes outer electrodes and CE denotes the central electrode.

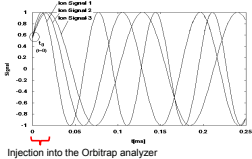


**FIGURE 3.** Illustration of synchronization of different  $m/z$ .

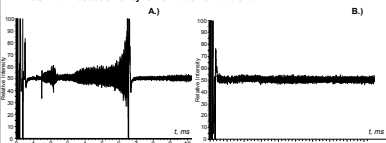


**FIGURE 4.** Improved stabilization of voltages allowed for a reduction in delay in the switching-on of the detection after ion injection from 8...9 ms (A) to < 0.6 ms (B).

## Enhanced FT

From  $t_0$  it is then possible to calculate  $\varphi_0$  for each component, i.e. the initial phase at that moment, and use it for determination of absorption  $A(p)$  and dispersion spectra  $D(p)$ :

$$\begin{pmatrix} A(p) \\ D(p) \end{pmatrix} = \begin{pmatrix} \cos \varphi_0 & \sin \varphi_0 \\ -\sin \varphi_0 & \cos \varphi_0 \end{pmatrix} \begin{pmatrix} \text{Re}(p) \\ \text{Im}(p) \end{pmatrix} \quad (4)$$

where  $\varphi_0 = \varphi_0 + \Delta\varphi$ . In the second approximation, there is a weak dependence of  $\varphi_0$  on  $m/z$  as shown in Figure 5. Both  $\varphi_0$  and  $t_0$  need to be calibrated within the eFT calibration procedure. In the current work, absorption and dispersion spectra were obtained using Flanning apodization and triple zero-filling [4]. Effects of these procedures on peak shape and spectral leakage are presented in Figure 6.

$A(p)$  and  $D(p)$  thus obtained can be used to calculate the enhanced FT spectrum  $ES(p)$  point-by-point:

$$ES(p) = ES(p)^{\text{absorbed}} + ES(p)^{\text{dispersed}} + ES(p)^{\text{combined}} \quad (5)$$

where

$$ES(p)^{\text{absorbed}} = C(p) \cdot A(p) + [-C(p)] \cdot M(p) \quad (6)$$

$M(p)$  is given by formula (1),

$$C(p) = 0.5 + 0.5 \cdot \left( \frac{A(p)}{\max(A(p))} - \frac{M(p)}{\max(M(p))} \right) \quad (7)$$

$\max(A(p))$  and  $\max(M(p))$  are local maxima of the corresponding spectra over the neighboring  $(2h+1)$  spectrum profile points calculated by 3-point parabolic interpolation. The quantity  $h$  is the number of neighboring points on either side of the point and in general,  $h$  will be of the order of the typical peak profile width (e.g.  $h=4$ ).

Second and third terms in (6) are used solely for further improvement of the side-lobe appearance. These corrections are calculated as a weighted sum of  $(2h-1)$  neighboring points following the method of 'finite-impulse-response' (FIR) filtering, as described in chapters 5 and 13 of [5].

$$ES(p)^{\text{absorbed}} = \sum_{k=-h}^{h-1} w_k \cdot A(p+k) \quad (8)$$

$$ES(p)^{\text{dispersed}} = \sum_{k=-h}^{h-1} w_k \cdot [-M(p+k)] \quad (9)$$

and  $k$  in (8)-(9) are the FIR coefficients which are typically pre-calculated, e.g. using simulated peaks in numerical experiments. The effect of this correction is illustrated in Figure 6.

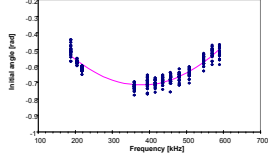


**FIGURE 5.** Dependence of  $\varphi_0$  on axial frequency of ions (and hence  $m/z$ ).

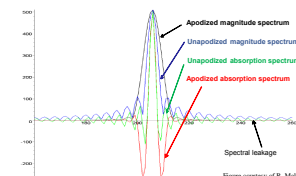


**FIGURE 6.** Effects of apodization on absorption and magnitude spectra. Drastic reduction of spectral leakage is clearly observed.

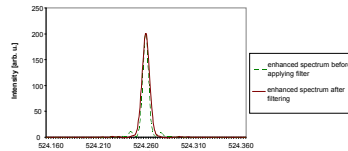


**FIGURE 7.** Effect of filtering on peak shape. Side-lobes of the peak are reduced significantly.

The center-of-mass of the peak is also calculated using a weighted average of absorption and magnitude spectra, with weighting shifted in favor of the latter.

Formula (5) was extensively tested on calibration mixtures, as well as different real-life samples, including complex peptide mixtures and standard proteins in LC/MS runs.

- Mechanism of ion injection into the Orbitrap-based mass spectrometers naturally provides inherent synchronization of ions of different  $m/z$ , which makes calculation of absorption spectra less demanding
- Improvements in detection circuitry were needed for eFT implementation
- Enhanced FT combines absorption and magnitude spectra in one enhanced spectrum, with peak shape improved by finite-impulse-response filtering

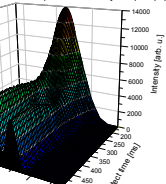
## Results

Figure 8 shows gradual separation of A+2 isotopes of MRFA peptide ( $C_{12}H_{16}N_2O_5S_8$  and  $C_{12}^{13}C_2H_{16}N_2O_5S_8$ ) in eFT spectra at increasing resolving power. The spectrum looks very similar to what the standard FT processing would provide from a twice longer transient.

Figure 9 shows that the gain from eFT depends on the decay of the signal and is reduced when the signal decays considerably during the acquisition time. In this case, resolution gain from eFT is not 2, but only +1.4 as predicted by a hard-sphere model [1]. Please note that for such rapidly decaying transients, apodization effects are quite noticeable for the standard mode of operation, but not in eFT mode.

Side-lobes of ion peaks obtained from enhanced spectra are typically within 1 to 3% of the main peak, which is the same order of the Gibbs-Oscillations that typical conventional Hann- or Hamming-windowed FTMS data shows. No baseline roll is observed. The elaborate dual-spectrum online processing is fast enough to cope with the LC/MS time scale, such cycle time is still determined by transient duration and ion injection times.

It was experimentally found that in the practical instrumentation accuracy of synchronization, and hence accuracy of calculation of absorption spectra is strongly dependent on any remaining jitter of electronics, dead time prior to the start of detection and signal-to-noise of peaks. The resulting mass accuracy of eFT thus appears to be similar to mass accuracy of traditional magnitude-mode FT even though peak width is halved. Figure 10 shows mass accuracy of eFT spectra in nano LC-MS/MS experiments of very complex peptide mixtures.



**FIGURE 8.** Separation of (A+2) isotope doublet peaks of MRFA peptide as detect time, and hence resolving power is increased until isobars are fully resolved.

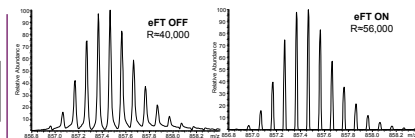


**FIGURE 9.** Spectrum for +10 charge state of Ubiquitin protein in the Thermo Scientific Q Exactive instrument from the 0.76 second acquisition, wherein transient decays with decay time of a few hundreds ms. Resolution gain from eFT is +1.4 as predicted by hard-sphere model [1].

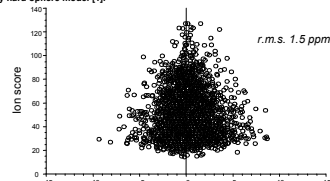


**FIGURE 10.** Mass accuracy of eFT spectra in nano LC-MS/MS experiments of very complex peptide mixtures. 1 µg E. Coli digest was separated by on-line nano-LC using a 30 min gradient. MS spectra were acquired with a data-dependent TOP10 HCD method consisting of a Full MS scan at 70,000 resolving power followed by a 10 data-dependent HCD spectra acquired at 17,500 resolution. The raw data file was searched using Thermo Scientific Proteome Discoverer software v. 1.3 with Mascot™ search engine and a precursor mass tolerance of 10 ppm.

## Conclusion

- Practical implementation of eFT indeed demonstrates up to 2-fold increase of resolving power for the same transient duration.
- The dual-spectrum online processing is fast enough to cope with the LC/MS time scale, such cycle time is essentially not influenced by eFT.
- Mass accuracy in eFT spectra is similar to that in traditional magnitude-mode FT spectra.
- Side-lobes in eFT spectra are comparable to those in conventional FT spectra.

## References

1. B. A. Vinberg, R. E. Bossio and A. G. Marshall, *Anal. Chem.*, 1999, 71 (2), pp 450-467.
2. S.C. Beu, G.T. Blakney, J.P. Quinn, C.L. Hendrickson, A.G. Marshall, *Anal. Chem.*, 2004, 76, pp 5756-5761.
3. Makarov A. "Theory and Practice of the Orbitrap Mass Analyzer", in book: *Practical Aspects of Trapped Ion Mass Spectrometry, Volume 4: Theory and Instrumentation* / Ed. R. E. March, J.F. Todd. CRC Press (Taylor & Francis), 2006.
4. A.G. Marshall, F.R. Verdun, *Fourier Transforms in NMR, Optical and Mass Spectrometry: A User's Handbook*. Elsevier, 1990.
5. Lyons R.G. (ed.), *Understanding Digital Signal Processing*. Prentice Hall, 2004.

## Acknowledgements

Authors would like to express their deep gratitude to Robert Malek, Hartmut Kuipers, Matthias Mueller, Stevan Horning, Jan-Peter Hauschild, Ulf Froehlich, Katharina Cron, and Markus Kellmann.

Mascot is a trademark of Matrix Science Ltd. All other trademarks are the property of Thermo Fisher Scientific and its subsidiaries. This information is not intended to encourage use of these products in any manner that might infringe the intellectual property rights of others.